ZMPSTE24 defends against influenza and other pathogenic viruses

ZMPSTE24 defends against influenza and other pathogenic viruses

Bishi Fu,[1]* Lingyan Wang,[2]* Shitao Li,[2] and Martin E. Dorf[1]

[1]Department of Microbiology and Immunobiology, Harvard Medical School, Boston, MA 02115
[2]Department of Physiological Sciences, Oklahoma State University, Stillwater, OK 74078

Zinc metallopeptidase STE24 (ZMPSTE24) is a transmembrane metalloprotease whose catalytic activity is critical for processing lamin A on the inner nuclear membrane and clearing clogged translocons on the endoplasmic reticulum. We now report ZMPSTE24 is a virus-specific effector that restricts enveloped RNA and DNA viruses, including influenza A, Zika, Ebola, Sindbis, vesicular stomatitis, cowpox, and vaccinia, but not murine leukemia or adenovirus. ZMPSTE24-mediated antiviral action is independent of protease activity. Coimmunoprecipitation studies indicate ZMPSTE24 can complex with proteins of the interferon-induced transmembrane protein (IFITM) family. IFITM proteins impede viral entry, and ZMPSTE24 expression is necessary for IFITM antiviral activity. In vivo studies demonstrate ZMPSTE24-deficient mice display higher viral burdens, enhanced cytokine production, and increased mortality after influenza infection. Collectively, these findings identify ZMPSTE24 as an intrinsic broad-spectrum antiviral protein and provide insights into antiviral defense mechanisms.

The Journal of Experimental Medicine

INTRODUCTION

Zinc metallopeptidase STE24 (ZMPSTE24) is a seven-spanner transmembrane-associated zinc metalloprotease. ZMPSTE24 homologues are found in many taxa, including bacteria, higher plants, and vertebrates. ZMPSTE24 enzymatic activity is also conserved, as indicated by the ability of human ZMP STE24 to complement enzymatic function of its counterpart in yeast (Leung et al., 2001; Ast et al., 2016). Functional complementation is supported by the nearly superimposable crystal structures of the yeast and human homologues (Pryor et al., 2013; Quigley et al., 2013). Mutations in the *zmpste24* gene that result in decreased enzyme function lead to a spectrum of diseases that share certain features of Hutchinson–Gilford progeria syndrome, including premature aging (Pegoraro et al., 2009; Young et al., 2014). Disease severity correlates with the residual enzymatic activity of mutant ZMPSTE24 (Barrowman et al., 2012). *Zmpste24*-deficient mice also develop a progeroid phenotype (Bergo et al., 2002; Pendás et al., 2002).

ZMPSTE24 is constitutively expressed and localizes to the inner nuclear membrane and cytoplasmic organelles. In mammals, ZMPSTE24 endoprotease activity is required for biogenesis of lamin A, which helps maintain the structural integrity of nuclear membranes (Bergo et al., 2002; Pendás et al., 2002; Michaelis and Barrowman, 2012). Additional studies demonstrated ZMPSTE24 catalytic activity removes misfolded proteins from clogged translocons. ZMPSTE24 and its yeast homologue were shown to protect the translocon by cleaving obtruding proteins, thereby maintaining homeostasis of the endoplasmic reticulum (Ast et al., 2016). ZMPSTE24 has promiscuous substrate specificity cleaving a heterogeneous spectrum of prenylated and nonprenylated targets (Ast et al., 2016; Hildebrandt et al., 2016).

Many enveloped viruses are ferried deep into the cytoplasm through endocytic vesicles and use the low pH endosomal environment to activate viral fusion proteins (Cossart and Helenius, 2014). Higher vertebrates evolved interferon-induced transmembrane protein (IFITM) family proteins to hinder endosomal penetration by fusogenic viruses (Brass et al., 2009; Perreira et al., 2013; Bailey et al., 2014). We now report the antiviral properties of IFITM are dependent on ZMPSTE24.

RESULTS AND DISCUSSION

ZMPSTE24 restricts viral infection, independent of its protease activity

HEK293 cells stably expressing C-terminal FLAG-tagged IFITM3 were stimulated with interferon. Affinity purification coupled with mass spectrometry (AP-MS) identified IFITM3-associated proteins. The significance analysis of interactome (SAINT) algorithm was adopted to analyze AP-MS data in combination with our reference database of FLAG-tagged protein complexes purified under identical conditions (Fu et al., 2015). 10 high-confidence interacting proteins including ZMPSTE24 with SAINT scores >0.89 were identified (Table S1).

*B. Fu and L. Wang contributed equally to this paper.

Correspondence to Martin E. Dorf: dorf@hms.harvard.edu; or Shitao Li: shitao.li@okstate.edu

Abbreviations used: AdV, adenovirus; AP-MS, affinity purification coupled with mass spectrometry; GLuc, *Gaussia* luciferase; IAV, influenza A virus; IFITM, interferon-induced transmembrane protein; Luc, firefly luciferase; MLV, murine leukemia virus; PR8, influenza A/Puerto Rico/8/1934 virus; SAINT, significance analysis of interactome; VACV, vaccinia virus; VLP, virus-like particle; VSV, vesicular stomatitis virus.

The Rockefeller University Press $30.00
J. Exp. Med. 2017 Vol. 214 No. 4 919–929
https://doi.org/10.1084/jem.20161270

Coimmunoprecipitation studies examined interactions between ZMPSTE24 and IFITM family proteins. ZMPSTE24 specifically binds IFITM1, IFITM2, or IFITM3 (Fig. 1 A). In contrast to IFITM, ZMPSTE24 transcription is not up-regulated by IFNβ stimulation (Fig. 1 B). To investigate the antiviral function of ZMPSTE24, HEK293 cells were transiently transfected with FLAG-tagged or control untagged ZMPSTE24 24 h before infection with influenza A/Puerto Rico/8/1934 virus (PR8) with *Gaussia* luciferase (GLuc; PR8-GLuc) reporter virus (Heaton et al., 2013). Both constructs inhibited influenza A virus (IAV) reporter activity (Fig. 1 C). Next, A549 lung cells were transfected with ZMPSTE24-FLAG; after 2 d, the cells were infected with PR8 IAV and examined by immunofluorescence. Ectopic expression of ZMPSTE24 limits and delays viral infection (Fig. 1 D). Furthermore, A549 cells expressing ZMPSTE24 produce fewer infectious IAV particles, as measured by plaque assay (Fig. 1 E).

To investigate viral specificity, ZMPSTE24 transfected cells were infected with vesicular stomatitis virus (VSV) carrying a firefly luciferase (Luc) gene (VSV-Luc; Cureton et al., 2012). ZMPSTE24 strongly inhibited VSV reporter activity (Fig. 1 F). Thus, the effect of ZMPSTE24 overexpression was tested on additional RNA viruses (Sindbis, murine leukemia virus [MLV], and Zika). ZMPSTE24 also inhibited Sindbis reporter activity, but not MLV (Fig. 1 F). Ectopic ZMPSTE24 expression also inhibits Zika infection in human T98-G glioblastoma cells (Fig. 1 G). Next, we examined the ability of ZMPSTE24 to restrict infection with three DNA viruses: adenovirus (AdV), vaccinia virus (VACV), and cowpox virus. Overexpression of ZMPSTE24 inhibited infection with VACV and cowpox virus, but not AdV (Fig. 1 F). As the IFITM sensitivity of pox viruses was not previously reported, we compared the ability of these viruses to infect *ifitmDel*$^{-/-}$ (deletion of *ifitm1*, *2*, *3*, *5*, and *6*) and reconstituted cells. The data indicate IFITM selectively protects against pox virus infection (Fig. 1 H).

To corroborate the role of ZMPSTE24 in antiviral defense, *zmpste24*$^{-/-}$ MEFs were examined. Plaque assays establish increased IAV production by *zmpste24*$^{-/-}$ cells (Fig. 2 A). To evaluate antiviral specificity, *zmpste24*$^{-/-}$ and *zmpste24*$^{+/+}$ MEFs were infected with VSV, Sindbis, MLV, VACV, cowpox, and AdV. Deficiency of ZMPSTE24 enhanced VSV, Sindbis, cowpox, and VACV reporter activity, but not MLV and AdV (Fig. 2 B). Importantly, reconstitution of *zmpste24*$^{-/-}$ MEFs with human ZMSPTE24 restored antiviral activity (Fig. 2 C). ZMPSTE24 knockdown also enhanced Zika virus replication in T98-G glioblastoma cells (Fig. 2 D). Finally, we examined the effects of ZMPSTE24 deficiency on primary human tracheal cells. RNAi depletion of ZMPSTE24 increased IAV, VSV, Sindbis, cowpox, and VACV infection in primary human respiratory epithelial cells (Fig. 2 E). To exclude RNAi off-target effects, cells were transfected with an siRNA-resistant ZMPSTE24 rescue construct before infection with PR8 reporter virus. The rescue construct restored antiviral activity, validating siRNA specificity (Fig. 2 F). The combined data suggest ZMPSTE24 restricts infection by selected RNA and DNA viruses.

To ascertain if enzymatic activity is critical for viral restriction, we mutated residues within the conserved HEXXH zinc metalloprotease motif, which is essential for catalytic activity (Pryor et al., 2013; Quigley et al., 2013). Wild type and mutants H335A and E336A exhibited comparable protection against IAV infection in A549 cells (Fig. 3 A). In addition, various ZMPSTE24 mutations identified from patients with reduced enzymatic activity (Barrowman et al., 2012) also displayed antiviral activity, with the exception of the L94P mutation, which lacked protein expression (Fig. 3 A). Furthermore, *zmpste24*$^{-/-}$ MEFs reconstituted with human ZMPSTE24 or the E336A catalytically inactive mutant restored host restriction to IAV, VSV, and VACV (Fig. 3 B). Collectively, the combined data suggest protease activity is not essential for ZMPSTE24 antiviral function.

ZMPSTE24 cooperates with IFITM to inhibit viral entry

Most enveloped viruses enter cells by breaching endosomal membrane barriers. To investigate the role of ZMPSTE24 in viral entry, we examined the effects of ZMPSTE24 overexpression on IAV release from endosomes. ZMPSTE24 restrained IAV release from highly acidic LysoTracker red–positive vesicles in A549 cells (Fig. 3 C). Furthermore, direct viral fusion assays using virus-like particles (VLPs) demonstrate *zmpste24*$^{-/-}$ cells are more susceptible to IAV viral entry than *zmpste24*$^{+/+}$ cells (Fig. 3 D). In contrast, ZMPSTE24 expression has no effect on entry of MLV particles (Fig. 3 D). *Zmpste24*$^{-/-}$ cells also demonstrated increased susceptibility to infection with VLP containing glycoproteins from HA1, HA5, or HA7 IAV, VSV, and Ebola (Fig. 3 E). Reciprocally, ZMPSTE24 overexpression inhibited entry of IAV, VSV, and Ebola VLP (Fig. 3 F). Collectively, the data suggest ZMPSTE24 impedes viral endosomal entry.

To establish the functional relationship between ZMPSTE24 and IFITM3, we performed genetic complementation experiments. Ectopic expression of IFITM3 does not restore antiviral function in *zmpste24*$^{-/-}$ cells (Fig. 3 B). However, ectopically expressed ZMPSTE24 restores antiviral activity against IAV, VSV, and VACV in *ifitmDel*$^{-/-}$ cells (Fig. 3 G). To determine whether ZMPSTE24 can still exert antiviral activity in the absence of IFITM, we silenced ZMPSTE24 in *ifitmDel*$^{-/-}$ MEFs. Notably, ZMPSTE24 knockdown uncovers an IFITM-independent restriction on VSV and VACV infection (Fig. 3 H). The combined results imply ZMPSTE24 is required for IFITM antiviral action, although the need for IFITM can be bypassed. The data are compatible with a model in which ZMPSTE24 serves as a downstream effector in the IFITM pathway, although an IFITM-independent pathway also exists.

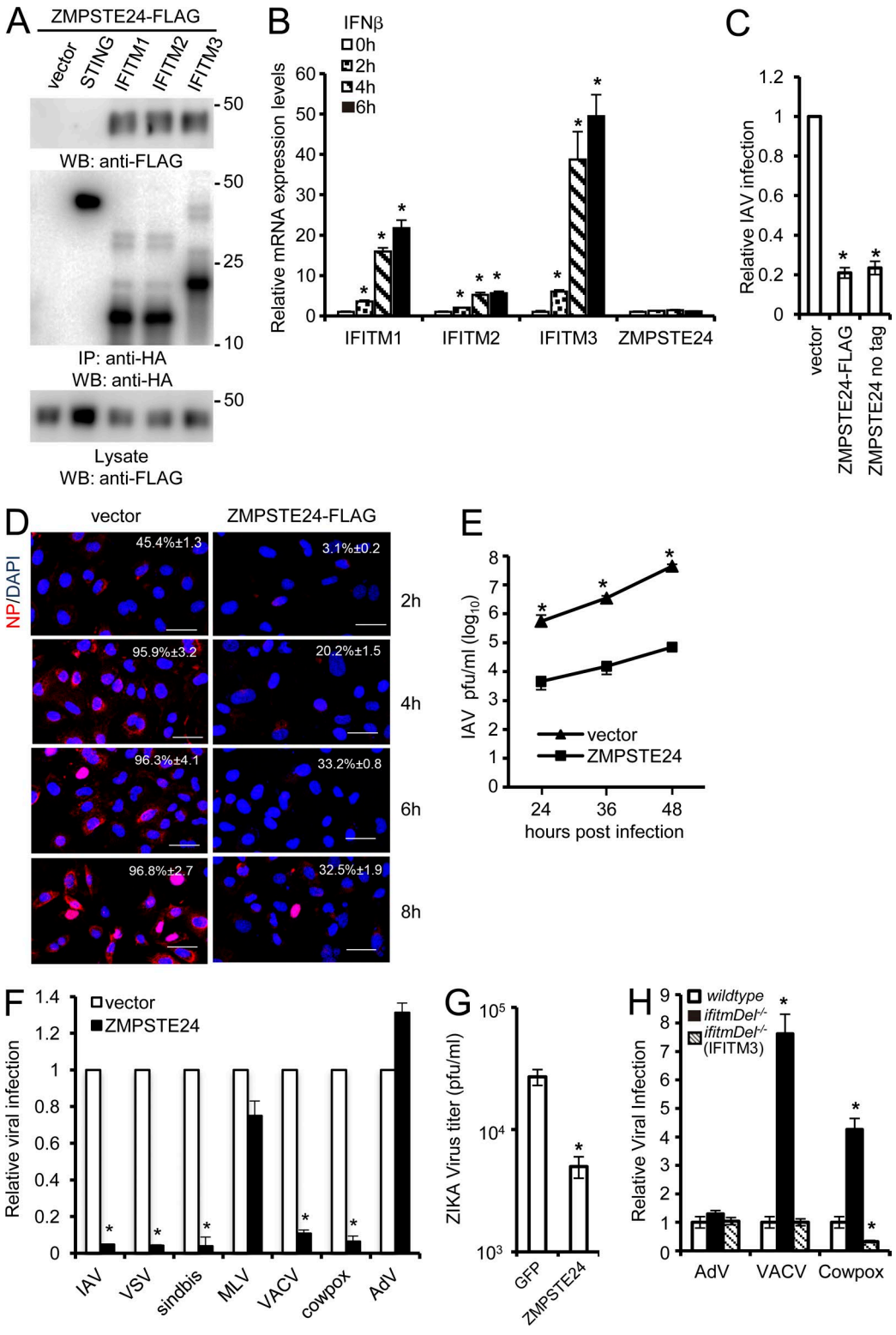

Figure 1. **ZMPSTE24 protects against viral infection.** (A) ZMPSTE24-FLAG was transfected with HA-tagged STING, IFITM1, IFITM2, or IFITM3 into HEK293 cells. After 48 h, cells were lysed and immunoprecipitated with anti-HA antibody and blotted with the indicated antibodies. Data are representative of two independent experiments. Molecular mass is indicated in kilodaltons. IP, immunoprecipitation; WB, Western blot. (B) A549 cells were stimulated with 5 U IFNβ for the designated times. IFITM1, IFITM2, IFITM3, ZMPSTE24, and control GAPDH mRNA levels were examined by real-time PCR (three independent experiments). Mean ± SD; *, $P < 0.05$. (C) Empty vector, ZMPSTE24-FLAG, or untagged ZMPSTE24 were transfected into HEK293 cells. After 24 h, cells were

ZMPSTE24 is required for influenza restriction in vivo

The progeria phenotype of *zmpste24*$^{-/-}$ mice can be complemented by reducing the level of prelamin A. *Zmpste24*$^{-/-}$ mice with half-normal levels of prelamin A are protected from disease (Fong et al., 2004, 2006; Varela et al., 2005; Mariño et al., 2008) and mount normal primary antibody responses after immunization with a limiting dose of IAV-derived HA protein (Fig. 4 A). To define the in vivo role of ZMPSTE24 on viral restriction, we compared antiviral responses of *lmna*$^{+/-}$*zmpste24*$^{-/-}$, *lmna*$^{+/-}$*zmpste24*$^{+/-}$, and *lmna*$^{+/-}$*zmpste24*$^{+/+}$ animals. ZMPSTE24-deficient mice displayed increased susceptibility to IAV with signs of severe clinical illness, including lethargy, hunched posture, and accelerated weight loss (Fig. 4 B). The weight loss in *zmpste24* heterozygous mice was intermediate, suggesting a gene dose effect (Fig. 4 B). 65% of *zmpste24*$^{-/-}$ animals became moribund (defined as 25% loss of body mass) compared with 20% and 0% in other groups (Fig. 4 C). IAV was detected in the lungs of all infected animals but did not spread to the spleen (Fig. 4 D). Lungs from ZMPSTE24-deficient mice exhibit the greatest increase in viral load. A gene dose effect was noted in the *zmpste24*$^{+/-}$ group (Fig. 4 D). Two days after infection, lungs from IAV-infected ZMPSTE24-deficient animals displayed focal areas of vasculitis and bronchitis with mixed polynuclear/mononuclear infiltrates and scattered areas of epithelial necrosis, whereas less pathology was noted in controls (Fig. 4 E). The histological findings were supported by increased levels of cytokines (IFNβ, TNF, and IL-6) and chemokines (MCP1/CCL2 and KC/CXCL1) in the lungs of IAV-infected *zmpste24*$^{-/-}$ animals (Fig. 4 F). After IAV infection, pulmonary IFITM3 expression was enhanced in *zmpste24*$^{-/-}$ and control mice. In contrast, ZMPSTE24 mRNA remained at constitutive levels after IAV infection (Fig. 4 G). The findings indicate ZMPSTE24 expression is not regulated by viral infection. The combined data suggest ZMPSTE24 deficiency is associated with enhanced viral proliferation and correspondingly more extensive tissue damage and imply ZMPSTE24-deficient mice are unable to control influenza infection.

In summary, ZMPSTE24 is an intrinsic antiviral protein that protects against pathogen attack. Of nine tested viruses, ZMPSTE24 selectively restricted infection by six distinct *viridae* families, representing diverse groups of enveloped RNA and DNA viruses. All ZMPSTE24-sensitive viruses require access to acidic endosomal compartments for viral entry. Representatives of each architectural class of fusogenic viral glycoprotein (Harrison, 2015) are susceptible to ZMPSTE24 inhibition, suggesting a common mechanism that alters endosomal trafficking or membrane structure rather than direct interaction with this varied assortment of virally encoded fusion proteins. Although we cannot exclude the possibility that ZMPSTE24 or IFITM associate with a common host-derived membrane element present in the viral envelop.

The best-characterized host restriction proteins involved in regulating viral entry are members of the IFITM family. ZMPSTE24 is detected in IFITM protein complexes and restricts a similar spectrum of RNA and DNA viruses. Genetic complementation experiments indicate ZMPSTE24 is required for IFITM antiviral activity, placing these two transmembrane proteins in a common pathway.

Viral endocytic entry is a complex process, involving endosomal trafficking, endosomal maturation, membrane bending, fluidity of membrane lipids, pre-hemifusion, and post-hemifusion events. Host proteins may interfere with different steps of the viral endocytic entry process. At the current stage, it is not clear which steps involve ZMPSTE24, how ZMPSTE24 antiviral activity is regulated, or whether other cofactors interact with ZMPSTE24. Nonetheless, ZMPSTE24 is an important element for innate host defense against a broad spectrum of pathogenic viruses.

MATERIALS AND METHODS

Mouse infection

Zmpste24$^{+/-}$ and *lmna*$^{+/-}$ animals on a C57BL background (N3 and N9, respectively) were purchased from Mutant Mouse Resource and Research Centers and The Jackson Laboratory, respectively. Intercrossed mice were maintained under specific pathogen–free conditions before infection. To avoid the complications of progeria, all experimental mice were heterozygous for the *lmna* gene (Fong et al., 2004, 2006; Varela et al., 2005; Mariño et al., 2008). Cohorts of age matched (2–4 mo) mice were anesthetized with 100 µg/g ketamine: 5 µg/g xylazine and then inoculated intranasally with 200 pfu influenza A/PR/8/34 in 20 µl sterile PBS. Weights were recorded daily as well as monitoring for signs of illness. Mice with 25% weight loss were considered moribund and euthanized. For histopathology, lungs from infected mice were fixed in Bouin solution (3 d) or 10% formalin (24 h) before transfer to 70% ethanol. Specimens were paraffin-embedded and stained by the Dana Farber/Harvard Cancer Center Histopathology

infected with 0.1 MOI PR8-GLuc for 16 h. Cell viability was determined by CellTiter-Glo, which was used for normalization (three experiments). Mean ± SD; *, P < 0.05. (D) A549 cells transfected with ZMPSTE24-FLAG (48 h) and then infected with 1 MOI PR8 for the indicated times (two experiments; percentage of positive cells from five fields ± SD are denoted). Bars, 100 µm. (E) A549 cells transfected with ZMPSTE24-FLAG were infected with 0.001 MOI WSN IAV for 12 h. Virus titers were determined by plaque assay. Data are representative of three experiments. Mean ± SD; *, P < 0.05. (F) A549 cells transfected with ZMPSTE24-FLAG were infected with 1 MOI IAV-GLuc, VSV-Luc, Sindbis-Luc, MLV-Luc, VACV-Luc, cowpox-Luc, and AdV5-Luc for 16 h (consolidated data). Each group was analyzed three times. Mean ± SD; *, P < 0.05. Viability assays of infected cells indicate <20% differences among groups. (G) GFP-FLAG or ZMPSTE24-FLAG was transfected in T98-G cells for 24 h before infection with 0.01 MOI MR 766 Zika virus. After 72 h, Zika virus titers were determined by plaque assay (three experiments). Mean ± SD; *, P < 0.05. (H) Wild-type, *ifitmDel*$^{-/-}$, and reconstituted MEFs were infected with 1 MOI AdV, VACV-Luc, or cowpox-Luc for 16 h. Relative luciferase activities were examined (three experiments). Mean ± SD; *, P < 0.05.

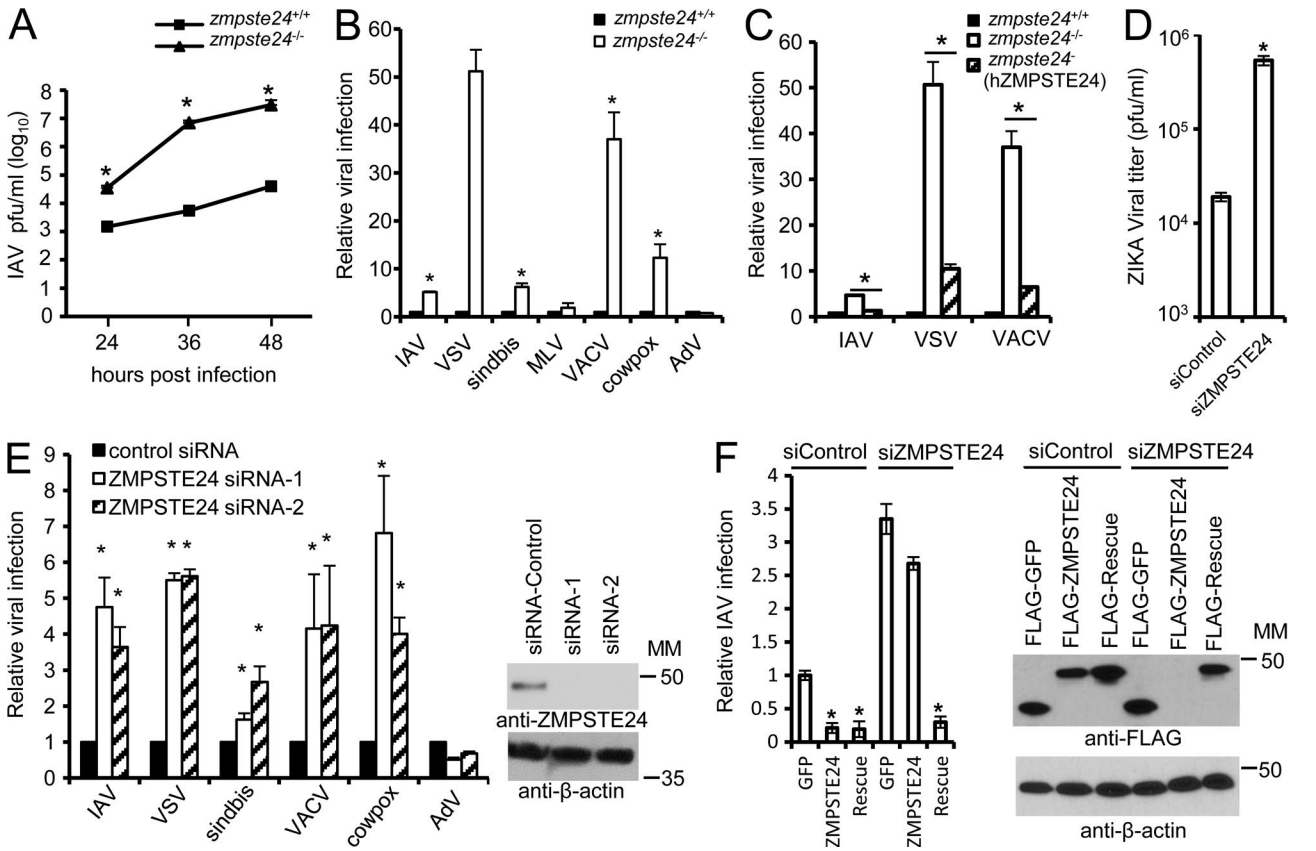

Figure 2. **ZMPSTE24 deficiency increases susceptibility to viral infection.** (A) *Zmpste24*$^{+/+}$ or *zmpste24*$^{-/-}$ MEFs were infected with 0.001 MOI WSN IAV for 12 h. Viral titers were determined by plaque assay (three experiments). Mean ± SD; *, P < 0.05. (B) *Zmpste24*$^{+/+}$ or *zmpste24*$^{-/-}$ MEFs infected with 1 MOI IAV-GLuc, VSV-Luc, Sindbis-Luc, MLV-Luc, VACV-Luc, cowpox-Luc, and AdV-Luc for 16 h (consolidated data). Each group was analyzed in three experiments. Mean ± SD; *, P < 0.05. Viability comparisons indicate <20% differences between control and ZMPSTE24-deficient groups. (C) *Zmpste24*$^{+/+}$, *zmpste24*$^{-/-}$, and *zmpste24*$^{-/-}$ MEFs expressing human ZMPSTE24 were infected with IAV-GLuc, VSV-Luc, and VACV-Luc for 16 h. Data from one of three experiments are shown. Mean ± SD; *, P < 0.05. (D) Control or ZMPSTE24 siRNA#1 were transfected in T98-G cells for 24 h before infection with 0.01 MOI MR 766 Zika virus. After 72 h, Zika virus titers were determined by plaque assay (three experiments). Mean ± SD; *, P < 0.05. (E) Primary human tracheal epithelial cells were transfected with ZMPSTE24 siRNAs (72 h) and then infected with the indicated luciferase-expressing viruses for 16 h. Data are from one of three experiments performed in triplicate. Mean ± SD; *, P < 0.05. Right panel depicts siRNA knockdown efficiency. (F) A549 cells were transfected with GFP-FLAG, ZMPSTE24-FLAG, rescue ZMPSTE24-FLAG, and control or ZMPSTE24 siRNA#1. After 48 h, cells were infected with 0.01 MOI PR8-GLuc for 16 h. The relative luciferase signal is shown. Western blot demonstrates expression levels. Data are from one of three experiments performed in triplicate. Mean ± SD; *, P < 0.05. (E and F) Molecular mass (MM) is indicated in kilodaltons.

core services. All experiments were performed with approval of Harvard Medical School, Committee on Animals.

Immunization

Animals were immunized s.c. in two sites with a total of 10 µg purified PR8-derived HA antigen (Sino Biologicals) precipitated with 2 mg magnesium hydroxide and 2 mg aluminum hydroxide.

Antibodies

Source, application, and dosage are indicated sequentially as follows: anti–β-actin (WB [1:1000]; Abcam), anti-FLAG (WB [1:1,000]; Sigma-Aldrich), anti-NP (IFA [1:1,000]; EMD Millipore), anti-HA epitope (WB [1:1,000]; Sigma-Aldrich), monoclonal anti-ZMPSTE24 antibody (described elsewhere; Pendás et al., 2002; WB [1:500]; gift from C. López-Otin, University of Oviedo, Oviedo, Spain), goat anti–rabbit IgG-HRP (WB [1:10,000]; Santa Cruz Biotechnology, Inc.), and Alexa Fluor 488 or 594 goat anti–mouse IgG (H+L, IFA [1:200]; Thermo Fisher Scientific).

Plasmids

Human ZMPSTE24, IFITM1, IFITM2, and IFITM3 cDNA were provided by the Dana Farber/Harvard Cancer Center DNA Resource Core. C-terminal epitope-tagged constructs were made by cloning into pCMV-3Tag-8 (Agilent Technologies). Mutations of ZMPSTE24-FLAG were constructed using the QuikChange II Site-Directed Mutagenesis kit

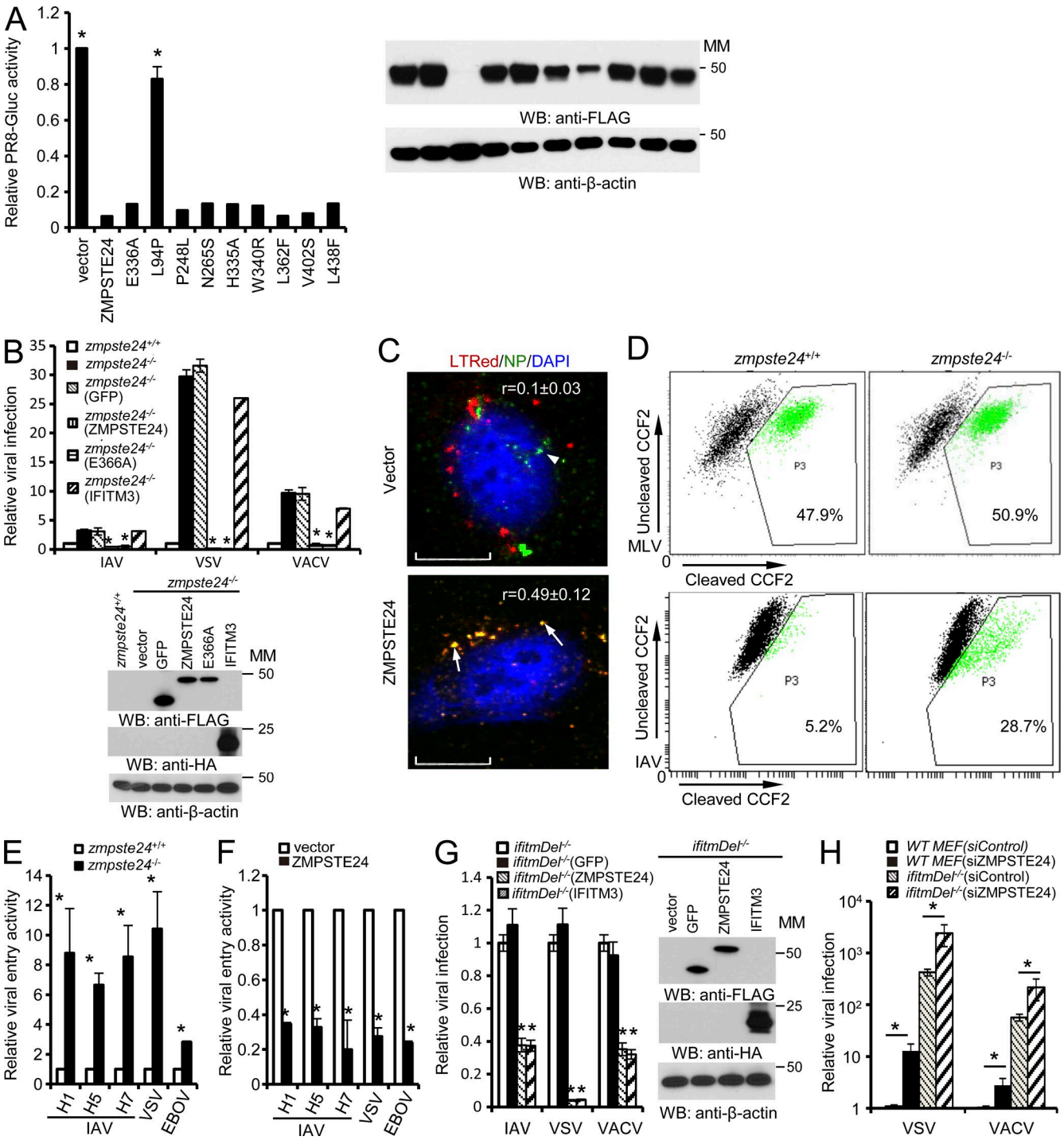

Figure 3. **ZMPSTE24 inhibits viral entry, but catalytic activity is dispensable for antiviral function.** (A) HEK293 cells were transfected with vector, ZMPSTE24-FLAG, or the indicated ZMPSTE24 mutants. After 24 h, cells were infected with 1 MOI PR8-GLuc for 16 h. Luciferase activity assays were performed. Each group was tested in three experiments. Mean ± SD; *, $P < 0.05$. (B) *Zmpste24*$^{+/+}$, *zmpste24*$^{-/-}$, and *zmpste24*$^{-/-}$ MEFs transduced with retrovirus expressing FLAG-tagged GFP, ZMPSTE24, E336A mutant ZMPSTE24, or IFITM3-HA were infected with IAV-GLuc, VSV-Luc, or VACV-Luc for 16 h. Relative luciferase levels are shown. Representative data from one of three experiments are shown. Mean ± SD; *, $P < 0.05$. Western blot demonstrates expression levels. (C) A549 cells transfected with ZMPSTE24 were infected with 50 MOI PR8 (2 h) and then stained with LysoTracker red, DAPI, and anti-NP. The arrowhead indicates nuclear localization of influenza NP protein. Arrows indicate representative colocalized puncta. Pearson's *r* coefficients are denoted. Bars, 10 µm. (D) *Zmpste24*$^{+/+}$ and *zmpste24*$^{-/-}$ cells were infected with IAV or MLV VLPs and then loaded with CCF2. Cleavage of CCF2 was determined by fluorescence emission shift from 520 nm (uncleaved CCF2) to 447 nm (cleaved CCF2). Data are representative of two experiments. (E) *Zmpste24*$^{+/+}$ and

(Agilent Technologies). For retroviral infection, ZMPSTE24-FLAG and IFITM3 were cloned into pQCXIP retroviral vector (Takara Bio Inc.). HEK293 cells were transfected using Lipofectamine 2000 Transfection Reagent, whereas A549 cells were transfected using Lipofectamine LTX Transfection Reagent (Thermo Fisher Scientific) according to the manufacturer's protocol. After 48 h, cells were ready for further treatment. IFITM3-HA and STING-HA constructs (Ishikawa and Barber, 2008; Brass et al., 2009) were gifts from A. Brass (University of Massachusetts Medical School, Worcester, MA) and G. Barber (University of Miami School of Medicine, Miami, FL), respectively.

Cells

HEK293 cells (ATCC), *ifitmDel*$^{-/-}$ MEFs (Brass et al., 2009; a gift from M. Farzan, Scripps Research Institute, Jupiter, FL), *zmpste24*$^{+/+}$ MEFs, and *zmpste24*$^{-/-}$ MEFs (Bergo et al., 2002; a gift from S. Young, University of California, San Francisco, San Francisco, CA) were maintained in DMEM containing antibiotics and 10% FBS. A549 and T98-G cells (ATCC) were cultured in RPMI Medium 1640 plus 10% FBS and 1× MEM nonessential amino acids solution. Primary human tracheal epithelial cells and supporting medium were purchased from Lifeline Technology.

Viruses

Influenza PR8-GLuc virus with a GLuc gene inserted downstream of PB2 was a gift from P. Palese (Mount Sinai School of Medicine, New York, NY; Heaton et al., 2013). IAV was propagated in specific pathogen-free fertilized eggs Premium Plus (Charles River) according to previously published protocols (Szretter et al., 2006). IAV was titered by plaque assay as described elsewhere (Matrosovich et al., 2006).

VSV-Luc was a gift from S. Whelan (Harvard Medical School, Boston, MA). VACV with Luc gene (VACV-Luc) was a gift from D.L. Bartlett (University of Pittsburg, Pittsburg, PA). Cowpox virus expressing luciferase was a gift from B. Moss (National Institutes of Health, Bethesda, MD). Sindbis virus carrying luciferase gene was a gift from R. Andino (University of California, San Francisco, San Francisco, CA) and J. Kagan (Children's Hospital, Boston, MA). VSV-Luc and VACV-Luc were expanded in BHK-21 cells. Adenovirus 5 with luciferase was purchased from the University of Iowa Viral Vector Core. Zika virus MR 766 was supplied by BEI Resources. For Zika plaque assays, Vero cells (ATCC) were grown to 90% confluence and then incubated with viral samples for 1 h at 37°C. Afterward, virus was removed and cells were washed with PBS. The cells were then covered with 2% methyl-cellulose in DMEM containing 2% FBS for 6 d and stained with crystal violet.

Reporter assay

For reporter virus assay, cells were counted using Countess Automated Cell Counter (Invitrogen), and equal numbers of cells were split into culture plates. 16 h later, cells were infected with indicated reporter virus for 16 h and then collected for reporter assay. Gaussia (New England BioLabs, Inc.) and Luc (dual-luciferase reporter assay; Promega) substrates were used as recommended by manufacturer. Each experiment was performed in triplicate. P-values were determined with paired Student's two-tailed *t* test. Cell number was assessed using the CellTiter-Glo Luminescent Cell Viability Assay (Promega).

Pseudotyped virus

For viral infection activity assay, pseudotyped viruses were generated by coexpression of indicated viral envelope construct and MSCV IRES luciferase (Addgene; donated by S. Lowe, Cold Spring Harbor, NY) in HEK293 cells. MSCV IRES luciferase plasmid was cotransfected with pCL-Ampho Retrovirus Packaging Vector (IMGENEX) into HEK293 cells to generate MLV-Luc pseudoviruses.

Entry assay using VLPs

The entry assay was based on a previously published protocol (Tscherne and García-Sastre, 2011) with minor modifications as follows. To prepare IAV VLPs, HEK 293 cells were transfected with β-lactamase M1 (BlaM1; β-lactamase was fused to WSN/33 M1 gene, a gift from A. Garcia-Sastre, Mount Sinai School of Medicine, New York, NY) and WSN/33 NA plus WSN/33 HA, or VN/2004 H5N1-HA or Anhui/2013 H7N9-HA. To make VLPs for VSV, HEK293 cells were transfected with BlaM1 and VSV-G. For preparation of the Zaire Ebola virus VLPs, BlaM-VP40 and Ebola glycoprotein (gifts from L. Rong, University of Illinois, Chicago, IL) were transfected into HEK293 cells. Medium containing influenza VLPs was treated with 2 μg/ml TPCK-trypsin for 30 min at 37°C to cleave HA. For preparation of MLV particles, MLV envelop (pHCMV-EcoEnv; Addgene) was cotransfected with BlaM-VP40 in HEK293 cells.

zmpste24$^{-/-}$ cells were infected with IAV (HA1, HA5, and HA7), VSV, and Ebola VLP (2 h) and then assayed for viral entry with CCF2. Data are representative of two or more experiments per group. Mean ± SD; *, P < 0.05. Percentages of positive *zmpste24*$^{+/+}$ MEFs were 5.2%, 3.8%, 3.4%, 5.6%, and 4.2%, respectively. (F) HEK293 cells were transfected with ZMPSTE24 for 24 h and then infected with the indicated VLPs. Data are representative of two or more experiments per group. Mean ± SD; *, P < 0.05. Percentages of infected cells in the vector transfected control group were 23%, 17%, 18%, 39%, and 26%, respectively. (G) *IfitmDel*$^{-/-}$ and *ifitmDel*$^{-/-}$ MEFs expressing GFP-FLAG, ZMPSTE24-FLAG, or IFITM3-HA were infected with 1 MOI PR8-GLuc, VSV-Luc, or VACV-Luc (16 h). Mean ± SD; *, P < 0.05. Western blot (WB) shows expression levels. Data are representative of two independent experiments. (A, B, and G) Molecular mass (MM) is indicated in kilodaltons. (H) IfitmDel$^{-/-}$ and wild-type MEFs were transfected with nontargeting control or ZMPSTE24 siRNA#2. After 48 h, cultures were infected with VSV-Luc or VACV-Luc reporter virus. Luciferase levels were monitored 16 h after infection (three experiments). Mean ± SD; *, P < 0.05.

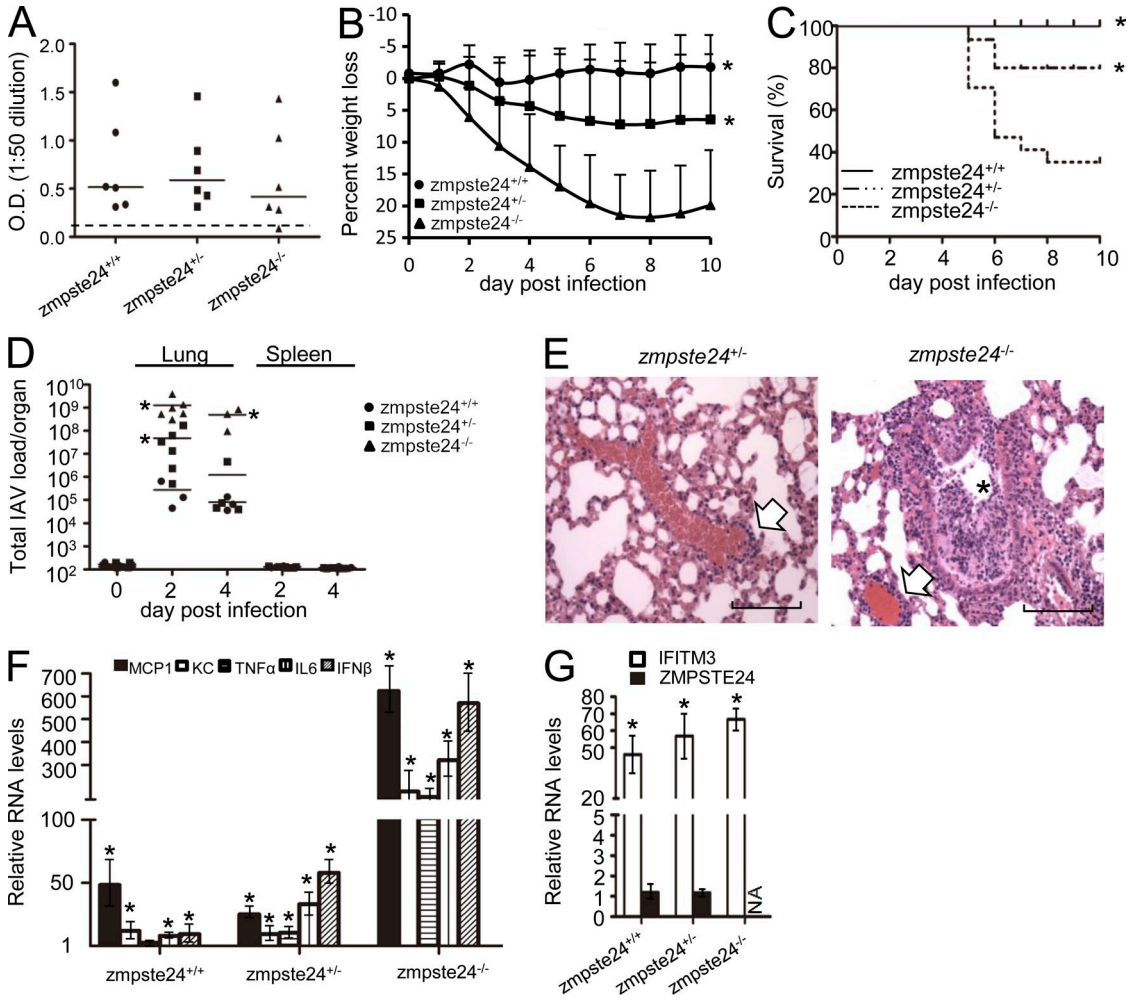

Figure 4. **ZMPSTE24 limits influenza infection in vivo.** (A) Primary antibody responses of *lmna*$^{+/-}$*zmpste24*$^{+/+}$, *lmna*$^{+/-}$*zmpste24*$^{+/-}$, and *lmna*$^{+/-}$*zmpste24*$^{-/-}$ mice (six animals per group) 13 d after immunization with purified PR8 HA protein. ELISA assay; OD of all preimmune sera were below the dashed line. (B) Percentage of loss in body mass ± SD of *lmna*$^{+/-}$*zmpste24*$^{+/+}$, *lmna*$^{+/-}$ *zmpste24*$^{+/-}$, and *lmna*$^{+/-}$*zmpste24*$^{-/-}$ mice after i.n. infection with 200 pfu PR8 IAV. Groups contained 5, 15, and 17 mice, respectively. Means are indicated by horizontal bars. *, P < 0.001 versus the *zmpste24*$^{-/-}$ group by Wilcoxon rank sum test; P < 0.001 for *zmpste24*$^{+/+}$ versus the *zmpste24*$^{+/-}$ group. (C) Survival curve of IAV-infected mice depicted in B. *, P < 0.05 versus *lmna*$^{+/-}$*zmpste24*$^{-/-}$ group by Mantel–Cox log-rank test. (D) Comparison of pulmonary and splenic IAV (NP) levels in uninfected and infected (2 or 4 d) *lmna*$^{+/-}$*zmpste24*$^{+/+}$, *lmna*$^{+/-}$*zmpste24*$^{+/-}$, and *lmna*$^{+/-}$*zmpste24*$^{-/-}$ animals (three to five mice per group) by quantitative PCR. Means ± SD are indicated by horizontal bars; *, P < 0.05. (E) Lung histopathology comparing *lmna*$^{+/-}$*zmpste24*$^{+/-}$ and *lmna*$^{+/-}$*zmpste24*$^{-/-}$ donors (2 d after IAV infection). Data are representative of three mice per group. Arrows point to regions of vasculitis with lymphocyte infiltrate. The asterisk illustrates region of suppurative bronchitis. Bars, 200 µm. (F) Relative increase in pulmonary RNA levels ± SD for cytokines (IL-6, TNF, and IFNβ) and chemokines (MCP1 and KC) in IAV-infected (day 2) mice (three to five animals per group) from D. Normalized to day 0 levels, the L32 housekeeping gene was used to establish comparable levels of RNA in all groups. *, P < 0.05. (G) IFITM3 and ZMPSTE24 mRNA expression in IAV-infected (day 2) lungs from D. Normalized to day 0 levels, the L32 housekeeping gene was used to normalize RNA levels. Mean ± SD; *, P < 0.05. NA indicates not applicable.

For fusion assays, HEK293 cells were seeded into 24-well plates and transfected with pCMV-Tag-4 vector or ZMPSTE24-FLAG. To infect *zmpste24*$^{+/+}$ and *zmpste24*$^{-/-}$ MEFs, cells were split into six-well plates and cultured in Opti-MEM. VLPs were added, and then plates were centrifuged for 60 min at 450 *g*, 4°C, followed by 2–4 h incubation at 37°C. To detect β-lactamase activity by flow cytometry, cells were detached with 0.1% trypsin/EDTA. Samples were gated on live cells for 10,000 events and analyzed for the emission of uncleaved CCF2 at 520 nm and cleaved CCF2 at 447 nm.

Immunoprecipitation

1×10^6 cells were lysed in 500 µl TAP lysis buffer (50 mM Tris-HCl [pH 7.5], 10 mM $MgCl_2$, 100 mM NaCl, 0.5% Nonidet P40, 10% glycerol, and Complete EDTA-free protease inhibitor cocktail tablets [Roche]) for 30 min at 4°C. Protein samples were heated at 60°C for 10 min. For im-

munoprecipitation, 2% of cell lysates (10^6 cells) were saved for input control, and the remainder was incubated with 10 µl EZview Red Anti-HA Affinity Gel (Sigma-Aldrich). After mixing end-over-end at 4°C overnight, the beads were washed three times (1 min per wash) with 500 µl lysis buffer. Anti-HA Affinity Gel was eluted with 50 µl of 1 mg/ml HA peptide (Sigma-Aldrich). AP-MS procedures and analyses are detailed elsewhere (Fu et al., 2015). Methods for AP-MS were described previously (Fu et al., 2015). SAINT scores were calculated following established procedures (Choi et al., 2011).

Immunofluorescence assay

Cells were cultured in the Lab-Tek II Chamber Slide with Cover CC2 Glass Slide Sterile (4 wells; Thermo Fisher Scientific). After indicated treatment, cells were fixed and permeabilized using cold methanol for 10 min at −20°C. The slides were then washed with PBS for 10 min and blocked with Odyssey Blocking Buffer (LI-COR Biosciences) for 1 h. Slides were incubated in Odyssey Blocking Buffer with appropriately diluted primary antibodies at 4°C for 16 h. After three washes (5 min per wash) with PBS, cells were incubated with corresponding Alexa Fluor–conjugated secondary antibodies (Thermo Fisher Scientific) for 1 h at room temperature. The slides were washed three times (5 min each time) with PBS and counter stained with 300 nM DAPI for 1 min, followed by PBS washing for 1 min. After air drying, slides were sealed with Gold Seal Cover Glass (Electron Microscopy Sciences) using Fluorogel (Electron Microscopy Sciences). Images were captured and analyzed using a FluoView confocal microscope (Olympus). At least 20 cells were analyzed in each experiment, and representative data from three experiments are presented.

Real-time PCR

Lungs and spleens were collected in 1 ml RNAlater (Ambion) and stored at −80°C. Specimens were homogenized using the TissueLyser II apparatus (QIAGEN). Total RNA was prepared using RNeasy columns (QIAGEN), after which the RNA was treated with RNase-free DNase to remove contaminating DNA. 1 µg RNA was transcribed into cDNA using QuantiTect reverse transcription kit (QIAGEN). For one real-time reaction, a 20 µl SYBR green PCR reaction mix (Roche) including 1/10 of the synthesized cDNA plus an appropriate oligonucleotide primer pair was run on the LightCycler 480 (Roche). The comparative Ct method was used to determine relative mRNA expression of genes as normalized by the housekeeping genes, GAPDH or L32. Primer sequences are listed in Table 1.

RNAi depletion

RNAi duplexes for human ZMPSTE24 (s20065 and s20066; Ambion) and mouse ZMPSTE24 (s20066; Ambion) were verified by RT-PCR. A549 and MEFs were transfected with siRNA duplexes using Lipofectamine RNAiMAX Transfection Reagent (Thermo Fisher Scientific) according to the manufacturer's protocol. Knockdown was allowed to proceed for 48 h before cells were infected or tested in functional assays.

ELISA

50 µl of 1 µg/ml PR8-derived HA antigen in borate buffer, pH 8.5, was coated onto 96-well MaxiSorp Immuno plates (Nalgene Nunc) overnight and then blocked with PBS containing 1% BSA and 0.05% Tween 20. 100 µl antisera diluted 1:50 in blocking buffer was added to each well and incubated for 1 h at room temperature. After three washes in PBS with 0.05% Tween 20, HRP-conjugated anti–mouse Ig (1:1,000; Invitrogen) was added for 1 h. After five rinses with PBS plus 0.05% Tween 20, 100 µl *o*-phenylenediamine dihydrochloride substrate solution (Sigma-Aldrich) was added for 25 min. The reaction was stopped with 100 µl 0.5 M H_2SO_4, and optical densities were read at 490 nm (Spectro Max Plus; Molecular Devices).

Table 1. **Primer sequences used in this study**

Target	Forward primer (5′–3′)	Reverse primer (5′–3′)
hZMPSTE24	TGTACCACCGGAGTTAGGACA	AGCCAGCATAACCACAGAACC
hIFITM1	ATCAACATCCACAGCGAGAC	CAACCATCTTCCTGTCCCTAG
hIFITM2	GATGTCCACCGTGATCCAC	CAACCATCTTCCTGTCCCTAG
hIFITM3	CCAACCATCTTCCTGTCCC	ATGTCGTCTGGTCCCTGTTC
mZMPSTE24	GCCTGGCTGTTCACATTAGTT	GGAACGCTTAGATCCTTCAACAA
hGAPDH	AGGTGAAGGTCGGAGTCA	GGTCATTGATGGCAACAA
mIL-6	TGGGGCTCTTCAAAAGCTCC	AGGAACTATCACCGGATCTTCAA
mIFNβ	CAGCTCCAAGAAAGGACGAAC	GGCAGTGTAACTCTTCTGCAT
mTNFα	TACTGAACTTCGGGGTGATTGGTCC	CAGCCTTGTCCCTTGAAGAGAACC
mKC	TGCACCCAAACCGAAGTCAT	TTGTCAGAAGCCAGCGTTCAC
mMCP1	ACCACAGTCCATGCCATCAC	TTGAGGTGGTTGTGGAAAAG
mL32	AAGCGAAACTGGCGGAAAC	TAACCGATGTTGGGCATCAG
mIFITM3	CCCCCAAACTACGAAAGAATCA	ACCATCTTCCGATCCCTAGAC
Rescue	CCGACTACATTGCCCCTTTATTTGAC	CGTAAATGGTGACAAGAACCAGAGAC
PR8 IAV NP	GCGTCTCAAGGCACCAAAC	TCAAAAGCAGAGAGCACCATT

Statistical analysis

Unless noted otherwise, statistical significance was determined by two-tailed Student's *t* test for two groups. Analyses with a probability value <0.05 were considered statistically significant.

Online supplemental material

Table S1, included as an Excel file, shows an AP-MS dataset.

ACKNOWLEDGMENTS

We thank Michael Berman for expert technical assistance; Stephen Young for zmpste24$^{-/-}$ and control MEFs; Michael Farzan for ifitmDel$^{-/-}$ MEFs; Peter Palese, Sean Whelan, David L. Bartlett, Bernard Moss, Raul Andino, and Jonathan Kagan for reporter viruses; Adolfo Garcia-Sastre for viral entry assay; Carlos López-Otin for anti-ZMPSTE24 antibody; and Abraham Brass, Glen Barber, Lijun Rong, and Scott Lowe for constructs. We thank Greg Melikian for valuable discussions.

This work was supported by National Institutes of Health grants R01-AI089829 (to M.E. Dorf), R01-AI121288 (to M.E. Dorf), and P20-GM103648 (to S. Li) and the Research Equipment and DevelopmentFund (to S. Li).

The authors declare no competing financial interests.

Submitted: 5 August 2016
Revised: 10 November 2016
Accepted: 25 January 2017

REFERENCES

Ast, T., S. Michaelis, and M. Schuldiner. 2016. The protease Ste24 clears clogged translocons. *Cell*. 164:103–114. http://dx.doi.org/10.1016/j.cell.2015.11.053

Bailey, C.C., G. Zhong, I.C. Huang, and M. Farzan. 2014. IFITM-family proteins: The cell's first line of antiviral defense. *Annu. Rev. Virol.* 1:261–283. http://dx.doi.org/10.1146/annurev-virology-031413-085537

Barrowman, J., P.A. Wiley, S.E. Hudon-Miller, C.A. Hrycyna, and S. Michaelis. 2012. Human ZMPSTE24 disease mutations: Residual proteolytic activity correlates with disease severity. *Hum. Mol. Genet.* 21:4084–4093. http://dx.doi.org/10.1093/hmg/dds233

Bergo, M.O., B. Gavino, J. Ross, W.K. Schmidt, C. Hong, L.V. Kendall, A. Mohr, M. Meta, H. Genant, Y. Jiang, et al. 2002. Zmpste24 deficiency in mice causes spontaneous bone fractures, muscle weakness, and a prelamin A processing defect. *Proc. Natl. Acad. Sci. USA*. 99:13049–13054. http://dx.doi.org/10.1073/pnas.192460799

Brass, A.L., I.C. Huang, Y. Benita, S.P. John, M.N. Krishnan, E.M. Feeley, B.J. Ryan, J.L. Weyer, L. van der Weyden, E. Fikrig, et al. 2009. The IFITM proteins mediate cellular resistance to influenza A H1N1 virus, West Nile virus, and dengue virus. *Cell*. 139:1243–1254. http://dx.doi.org/10.1016/j.cell.2009.12.017

Choi, H., B. Larsen, Z.Y. Lin, A. Breitkreutz, D. Mellacheruvu, D. Fermin, Z.S. Qin, M. Tyers, A.C. Gingras, and A.I. Nesvizhskii. 2011. SAINT: probabilistic scoring of affinity purification-mass spectrometry data. *Nat. Methods.* 8:70–73. http://dx.doi.org/10.1038/nmeth.1541

Cossart, P., and A. Helenius. 2014. Endocytosis of viruses and bacteria. *Cold Spring Harb. Perspect. Biol.* 6:a016972. http://dx.doi.org/10.1101/cshperspect.a016972

Cureton, D.K., R. Burdeinick-Kerr, and S.P. Whelan. 2012. Genetic inactivation of COPI coatomer separately inhibits vesicular stomatitis virus entry and gene expression. *J. Virol.* 86:655–666. http://dx.doi.org/10.1128/JVI.05810-11

Fong, L.G., J.K. Ng, M. Meta, N. Coté, S.H. Yang, C.L. Stewart, T. Sullivan, A. Burghardt, S. Majumdar, K. Reue, et al. 2004. Heterozygosity for Lmna deficiency eliminates the progeria-like phenotypes in Zmpste24-deficient mice. *Proc. Natl. Acad. Sci. USA*. 101:18111–18116. http://dx.doi.org/10.1073/pnas.0408558102

Fong, L.G., J.K. Ng, J. Lammerding, T.A. Vickers, M. Meta, N. Coté, B. Gavino, X. Qiao, S.Y. Chang, S.R. Young, et al. 2006. Prelamin A and lamin A appear to be dispensable in the nuclear lamina. *J. Clin. Invest.* 116:743–752. http://dx.doi.org/10.1172/JCI27125

Fu, B., L. Wang, H. Ding, J.C. Schwamborn, S. Li, and M.E. Dorf. 2015. TRIM32 senses and restricts influenza A virus by ubiquitination of PB1 polymerase. *PLoS Pathog.* 11:e1004960. http://dx.doi.org/10.1371/journal.ppat.1004960

Harrison, S.C. 2015. Viral membrane fusion. *Virology.* 479-480:498–507. http://dx.doi.org/10.1016/j.virol.2015.03.043

Heaton, N.S., V.H. Leyva-Grado, G.S. Tan, D. Eggink, R. Hai, and P. Palese. 2013. In vivo bioluminescent imaging of influenza A virus infection and characterization of novel cross-protective monoclonal antibodies. *J. Virol.* 87:8272–8281. http://dx.doi.org/10.1128/JVI.00969-13

Hildebrandt, E.R., B.T. Arachea, M.C. Wiener, and W.K. Schmidt. 2016. Ste24p mediates proteolysis of both isoprenylated and non-prenylated oligopeptides. *J. Biol. Chem.* 291:14185–14198. http://dx.doi.org/10.1074/jbc.M116.718197

Ishikawa, H., and G.N. Barber. 2008. STING is an endoplasmic reticulum adaptor that facilitates innate immune signalling. *Nature.* 455:674–678. http://dx.doi.org/10.1038/nature07317

Leung, G.K., W.K. Schmidt, M.O. Bergo, B. Gavino, D.H. Wong, A. Tam, M.N. Ashby, S. Michaelis, and S.G. Young. 2001. Biochemical studies of Zmpste24-deficient mice. *J. Biol. Chem.* 276:29051–29058. http://dx.doi.org/10.1074/jbc.M102908200

Mariño, G., A.P. Ugalde, N. Salvador-Montoliu, I. Varela, P.M. Quirós, J. Cadiñanos, I. van der Pluijm, J.M. Freije, and C. López-Otín. 2008. Premature aging in mice activates a systemic metabolic response involving autophagy induction. *Hum. Mol. Genet.* 17:2196–2211. http://dx.doi.org/10.1093/hmg/ddn120

Matrosovich, M., T. Matrosovich, W. Garten, and H.D. Klenk. 2006. New low-viscosity overlay medium for viral plaque assays. *Virol. J.* 3:63. http://dx.doi.org/10.1186/1743-422X-3-63

Michaelis, S., and J. Barrowman. 2012. Biogenesis of the *Saccharomyces cerevisiae* pheromone a-factor, from yeast mating to human disease. *Microbiol. Mol. Biol. Rev.* 76:626–651. http://dx.doi.org/10.1128/MMBR.00010-12

Pegoraro, G., N. Kubben, U. Wickert, H. Göhler, K. Hoffmann, and T. Misteli. 2009. Ageing-related chromatin defects through loss of the NURD complex. *Nat. Cell Biol.* 11:1261–1267. http://dx.doi.org/10.1038/ncb1971

Pendás, A.M., Z. Zhou, J. Cadiñanos, J.M. Freije, J. Wang, K. Hultenby, A. Astudillo, A. Wernerson, F. Rodríguez, K. Tryggvason, and C. López-Otín. 2002. Defective prelamin A processing and muscular and adipocyte alterations in Zmpste24 metalloproteinase-deficient mice. *Nat. Genet.* 31:94–99.

Perreira, J.M., C.R. Chin, E.M. Feeley, and A.L. Brass. 2013. IFITMs restrict the replication of multiple pathogenic viruses. *J. Mol. Biol.* 425:4937–4955. http://dx.doi.org/10.1016/j.jmb.2013.09.024

Pryor, E.E. Jr., P.S. Horanyi, K.M. Clark, N. Fedoriw, S.M. Connelly, M. Koszelak-Rosenblum, G. Zhu, M.G. Malkowski, M.C. Wiener, and M.E. Dumont. 2013. Structure of the integral membrane protein CAAX protease Ste24p. *Science.* 339:1600–1604. http://dx.doi.org/10.1126/science.1232048

Quigley, A., Y.Y. Dong, A.C. Pike, L. Dong, L. Shrestha, G. Berridge, P.J. Stansfeld, M.S. Sansom, A.M. Edwards, C. Bountra, et al. 2013. The structural basis of ZMPSTE24-dependent laminopathies. *Science.* 339:1604–1607. http://dx.doi.org/10.1126/science.1231513

Szretter, K.J., A.L. Balish, and J.M. Katz. 2006. Influenza: Propagation, quantification, and storage. *Curr. Protoc. Microbiol.* Chapter 15:Unit 15G.1. http://dx.doi.org/https://10.1002/0471729256.mc15g01s3

Tscherne, D.M., and A. García-Sastre. 2011. An enzymatic assay for detection of viral entry. *Curr. Protoc. Cell Biol.* Chapter 26:Unit 26.12. http://dx.doi.org/https://10.1002/0471143030.cb2612s51

Varela, I., J. Cadiñanos, A.M. Pendás, A. Gutiérrez-Fernández, A.R. Folgueras, L.M. Sánchez, Z. Zhou, F.J. Rodríguez, C.L. Stewart, J.A. Vega, et al. 2005. Accelerated ageing in mice deficient in Zmpste24 protease is linked to p53 signalling activation. *Nature.* 437:564–568. http://dx.doi.org/10.1038/nature04019

Young, S.G., H.J. Jung, J.M. Lee, and L.G. Fong. 2014. Nuclear lamins and neurobiology. *Mol. Cell. Biol.* 34:2776–2785. http://dx.doi.org/10.1128/MCB.00486-14